



ELSEVIER

Journal of Materials Processing Technology 102 (2000) 33–39

Journal of  
**Materials  
Processing  
Technology**

www.elsevier.com/locate/jmatprotec

# Modeling of solidification in twin-roll strip casting

C.A. Santos, J.A. Spim Jr., A. Garcia\*

*Materials Engineering Department, State University of Campinas, PO Box 6122, 13083-970, Campinas, SP, Brazil*

Received 28 September 1998

## Abstract

Twin-roll continuous casting combines solidification and hot rolling into a single operation to produce thin strips that are directly coilable. It offers advantages of low capital investment and low operational cost, and the strips produced have a refined solidification microstructure, which has attracted interest of global metal producers. This is evidenced by numerous pilot-scale casters constructed. The successful development of near-net-shape casting depends critically on an understanding of the fundamental knowledge of heat and fluid flow. Despite sophisticated instrumentation technology, information critical to the understanding of the casting region cannot be measured directly, therefore it is necessary to develop efficient numerical tools to control the process. This paper presents a numerical model for the two-dimensional solidification problem in the twin-roll continuous casting system by using a finite difference technique. The thermal analysis results give valuable insight into the thermal characteristics of solidification and processing for the strip casting. Results of subsequent simulations are compared with data from the literature. © 2000 Elsevier Science S.A. All rights reserved.

*Keywords:* Strip casting; Twin-roll; Solidification; Mathematical modeling

## 1. Introduction

The maturity of conventional continuous casting and the large knowledge-base developed over recent years has permitted the development of a new generation of “near-net-shape” processes to produce thin slabs. Such processes reduce production costs, and energy, and require low capital investment when compared to conventional processes [1,2].

The “twin-roll” process (thin strips of 0.1–60 mm thickness) produces coilable strip directly from the melt by combining casting and hot rolling into a single step [3,4]. The principle is based on pouring the melt into the gap between two rotating water-cooling cylindrical copper rolls. The metal solidifies just before reaching the bite of the rolls and is then rolled as it passes through the rolls [5–7].

Amongst other metallurgical aspects typical of this process, the high freezing rate provides an extremely refined solidification microstructure characterized by dendritic ramifications, improves segregation and increases the mechanical properties of metal [8,9].

A schematic diagram of the twin-roll process as well as of pool aspects is shown in Fig. 1. As the “twin-roll” process

produces very thin strips, it needs high speeds of production to be competitive with conventional continuous-casting methods. Although this process presents various advantages, it is necessary to develop efficient numerical tools to elucidate the complicated flow and the heat-transfer mechanism, which will be specially useful for designing the optimum “twin-roll” systems [1,2,10].

The aim of this paper is to develop a heat-transfer mathematical model which must be able to analyze the metal/roll thermal behavior during the “twin-roll” process, using a finite difference technique. The model has input parameters such as the strip thickness, the gap between rolls, the roll speed, and the thermophysical properties of the rolls and the metal.

## 2. Mathematical formulation

### 2.1. Physical assumptions

The mathematical model was developed using a finite difference technique and permits the description of the evolution of liquidus and solidus isotherms and temperature gradients along the process. It was developed under a set of physical assumptions, listed below.

\* Corresponding author. Tel.: +55-19-788-3309; fax: +55-19-289-3722.  
E-mail address: amaurig@fem.unicamp.br (A. Garcia)

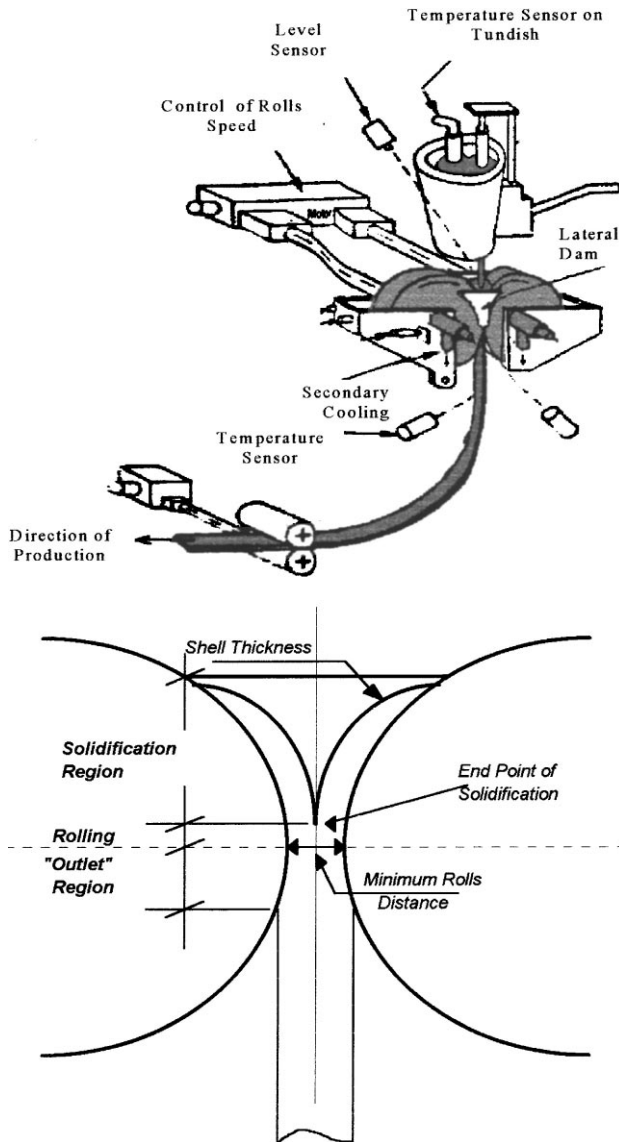


Fig. 1. A schematic diagram of the “twin-roll” process, emphasizing pool aspects.

1. The rolls do not deform and rotate at the same speed; and the temperature fields have mirror symmetry with respect to the center line between the rolls  $\partial T / \partial x|_{x=0} = 0$ ;
2. The inflow conditions of the temperature of the molten metal at the inlet are:

$$T = T_v, \quad v_x = 0, \quad v_y = \omega t_{in}$$

where  $v$  is the component of velocity in the  $x$  and  $y$  directions and  $w$  is the rotational speed of the roll;

3. The conditions at the exit are:

$$v_x = 0, \quad v_y = \omega f(t)$$

where  $f(t)$  is a step function;

4. On the outer surface of roll, the interfacial velocity is the speed of the roll or the casting speed:

$$v_x = 0, \quad v_y = \omega t_{out}$$

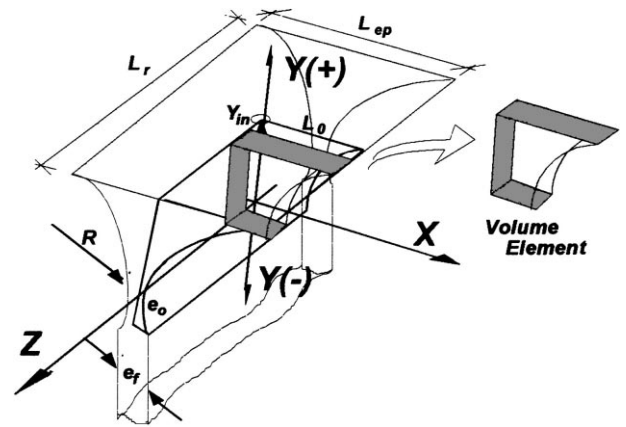


Fig. 2. Schematic diagram of the physical system and the volume element.

5. Heat conduction in the direction  $z$  is neglected. The volume element is positioned from the center of the pool (Fig. 2);
6. The thermophysical properties of the metal ( $\rho$  — density,  $c$  — specific heat,  $k$  — thermal conductivity) are variables with temperature in the mushy zone,  $f_s$  is variable with the temperature:

$$k = (k_s - k_l)f_s + k_l,$$

$$c = (c_s - c_l)f_s + c_l - (\rho L * \partial f_s / \partial t),$$

$$\rho = (\rho_s - \rho_l)f_s + \rho_l$$

7. The latent heat evolution ( $L$ ) along the solidification range is calculated using the equilibrium lever rule and Scheil’s formulation;
8. The metal/roll heat-transfer coefficient ( $h_0$ ) is assumed constant; and
9. The level of the molten metal is kept constant. In the case of a constant mass flow rate the following Peclet numbers, which represent the roll speed, are defined:

$$Pe_s = \frac{\omega R_{roll}}{\alpha_s}, \quad Pe_l = \frac{\omega R_{roll}}{\alpha_l}$$

where  $R$  is the roll radius and  $\alpha$  is the thermal diffusivity.

Fig. 2 shows a schematic three-dimensional representation of the liquid metal pool, as well as the coordinate system  $(x, y, z)$ , where  $L_{ep}$  is the pool thickness in the  $X$ – $Y$  plane,  $L_r$  the pool width in the  $Y$ – $Z$  plane,  $Y_{in}$  the pool height,  $R_{Roll}$  the roll radius,  $e_o$  the minimum distance between the rolls, and  $e_f$  is the final strip thickness.

### 2.2. Heat-transfer during solidification

The development of the model is based on the one-dimensional heat-conduction equation, given by

$$\rho c \frac{\partial T}{\partial t} = \frac{\partial}{\partial x} \left[ k(T) \frac{\partial T}{\partial x} \right] + \dot{q} \tag{1}$$

assuming an isotropic material, where

$\partial T/\partial t$  is the freezing rate and  $\dot{q}$  is the heat source associated with phase change, given by

$$\dot{q} = \rho L \frac{\partial f_s}{\partial t} \tag{2}$$

and  $L$  is the latent heat of fusion.

The solid fraction ( $f_s$ ), depends on a number of parameters involved in the system. However, it is quite reasonable to assume that  $f_s$  varies only with temperature.

The value of  $f_s$  can be obtained, amongst other formulations, from [11]:

$$f_s = \left( \frac{1}{1 - k_0} \right) \left[ \frac{T_1 - T}{T_f - T} \right] \text{ Lever rule} \tag{3}$$

$$f_s = 1 - \left( \frac{T_f - T}{T_f - T_1} \right)^{1/(k_0 - 1)} \text{ Scheil's equation} \tag{4}$$

$$f_s \Rightarrow \begin{cases} 0 & T > T_{\text{liquidus}} \\ 0 < f_s < 1 & \text{Lever ruler/Scheil's equation} \\ 1 & T < T_{\text{solidus}} \end{cases}$$

and by utilizing the concept of pseudo-specific heat ( $c'$ ), the following is obtained:

$$c' = c - L \frac{\partial f_s}{\partial T} \tag{5}$$

after which  $c$  can be substituted for  $c'$  in Eq. (1).

The model permits the insertion of physical properties as a function of temperature, considering the amount of solid and liquid fractions, as shown in Table 1, where,  $T_s$  is the solidus temperature,  $T_l$  the liquidus temperature and indices  $s$  and  $l$  indicate solid and liquid, respectively.

### 2.3. Finite difference representation of the heat conduction equation

Introducing finite-difference terms into Eq. (1), yields [12]:

$$\rho c' \frac{T_i^{n+1} - T_i^n}{\Delta t} = k \left( \frac{T_{i+1}^{n+1} - 2T_i^{n+1} + T_{i-1}^{n+1}}{\Delta x^2} \right) \tag{6}$$

where

$$T_i^{n+1} = T(t_i + \Delta t, x_i) \tag{7}$$

$$T_i^n = T(t_i, x_i) \tag{8}$$

$$T_{i+1}^{n+1} = T(t_i + \Delta t, x_i + \Delta x) \tag{9}$$

$$T_{i-1}^{n+1} = T(t_i + \Delta t, x_i - \Delta x) \tag{10}$$

Table 1  
Physical properties considered in the model calculations

Physical properties	Solid ( $T < T_s$ )	Liquid ( $T > T_l$ )	Solidification range ( $T_s < T < T_l$ )
Thermal conductivity ( $k$ )	$k_s$	$k_l$	$(k_s - k_l)f_s + k_l$
Density ( $\rho$ )	$\rho_s$	$\rho_l$	$(\rho_s - \rho_l)f_s + \rho_l$
Specific heat ( $c$ )	$c_s$	$c_l$	$(c_s - c_l)f_s + c_l - \rho \cdot L(\partial f_s / \partial T)$

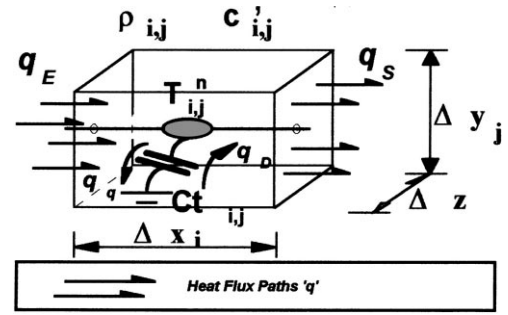


Fig. 3. Physical representation of thermal flux.

and  $t_i$  and  $x_i$  are instantaneous time and space representations.

Multiplying Eq. (6) by “ $\Delta x \Delta y \Delta z$ ” and considering  $\Delta t_x = \Delta y \Delta z$ :

$$\Delta x \Delta y \Delta z \rho c' \frac{T_i^{n+1} - T_i^n}{\Delta t} = \Delta t_x k \frac{(T_{i+1}^{n+1} - T_i^{n+1})}{\Delta x} + \Delta t_x k \frac{(T_{i-1}^{n+1} - T_i^{n+1})}{\Delta x} \tag{11}$$

Eq. (11) represents the variation of heat flux with time.

### 2.4. Analogy between electrical and thermal circuits and the FDM numerical technique applied to the heat flow phenomena

There is a large body of literature dealing with the basic relationship of the analogy between a thermal system and the passive elements of an electrical circuit (resistors and capacitors — Figs. 3 and 4):

$$Ct_i = \rho_i c'_i \text{Vol}_i \tag{12}$$

where  $\text{Vol}_i = \Delta x_i \Delta y_i \Delta z$

It can be seen from Eq. (11), that each term on the right-hand side is related to an equation similar to that which defines the thermal resistance  $Rt_{i,j}$  (Eq. (14)), in the following manner:

$$\Delta t_x k \frac{(T_{i+1}^{n+1} - T_i^{n+1})}{\Delta x} = \frac{(T_{i+1}^{n+1} - T_i^{n+1})}{Rt_{i \rightarrow i+1}} \tag{13}$$

where the term  $Rt_{i \rightarrow i+1}$  represents the thermal resistance at the heat flux line from point “ $i+1$ ” to point “ $i$ ”. This term is given by the sum of the thermal resistances inside

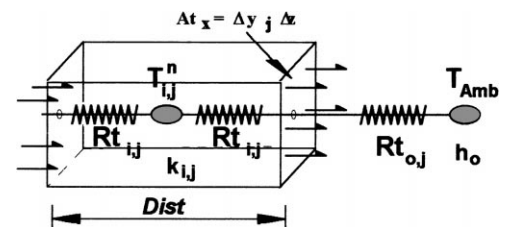


Fig. 4. Physical representation of thermal resistances.

the element “*i*” (from the center to the  $At_x$  interface) and the thermal resistances inside element “*i+1*” (from the  $At_x$  interface to the center), according to the following equation

$$Rt_{i-i+1} = Rt_i + Rt_{i+1} = \frac{\Delta x_i}{2k_i At_x} + \frac{\Delta x_{i+1}}{2k_{i+1} At_x} \quad (14)$$

The right-hand side terms of Eq. (14) can be re-arranged into the form:

$$Rt_{i-i+1} = \frac{1}{2At_x} \left( \frac{\Delta x_i}{k_i} + \frac{\Delta x_{i+1}}{k_{i+1}} \right) = \frac{1}{2At_x} \frac{k_{i+1}\Delta x_i + k_i\Delta x_{i+1}}{k_{i+1}k_i} \quad (15)$$

The mean thermal conductivity between points “*i+1*” (“*k<sub>i+1</sub>*”) and “*i*” (“*k<sub>i</sub>*”), “*k<sub>m</sub>*”, can be defined as

$$k_m = \frac{k_{i+1}\Delta x_i + k_i\Delta x_{i+1}}{k_{i+1}k_i} \quad (16)$$

A similar procedure makes it possible to find each term of Eq. (6), resulting in

$$\frac{Ct_i}{\Delta t} (T_i^{n+1} - T_i^n) = \frac{T_{i+1}^{n+1}}{Rt_i + Rt_{i+1}} + \frac{T_{i-1}^{n+1}}{Rt_i + Rt_{i-1}} - T_i^{n+1} \left( \frac{1}{Rt_i + Rt_{i+1}} + \frac{1}{Rt_i + Rt_{i-1}} \right) \quad (17)$$

By re-arranging Eq. (17):

$$T_i^n = -\frac{\Delta t}{\tau_{i+1}} T_{i+1}^{n+1} - \frac{\Delta t}{\tau_{i-1}} T_{i-1}^{n+1} + \left( 1 + \frac{\Delta t}{\tau_i} \right) T_i^{n+1} \quad (18)$$

where

$$\tau_{i+1} = Ct_i(Rt_{i+1} + Rt_i) \quad (19)$$

$$\tau_{i-1} = Ct_i(Rt_{i-1} + Rt_i) \quad (20)$$

$$\frac{1}{\tau_i} = \frac{1}{\tau_{i+1}} + \frac{1}{\tau_{i-1}} \quad (21)$$

Eq. (18) represents the implicit form of the finite difference method. The equation representing the explicit form is obtained by a similar treatment and is given by

$$T_i^{n+1} = \frac{\Delta t}{\tau_{i+1}} T_{i+1}^n + \frac{\Delta t}{\tau_{i-1}} T_{i-1}^n + \left( 1 - \frac{\Delta t}{\tau_i} \right) T_i^n \quad (22)$$

Eq. (22) becomes unstable for  $\Delta t \leq \tau_{i,j}$  (stability limits).

The thermal resistance at the heat flux line from point *i+1* to point *i* is given by

$$Rt_i = \frac{\Delta x}{k_i At} \quad (23a)$$

For the mesh elements in contact with the rolls, the thermal resistance is:

$$Rt_0 = \frac{1}{h_0 At} \quad (23b)$$

where  $h_0$  is the metal/roll heat-transfer coefficient.

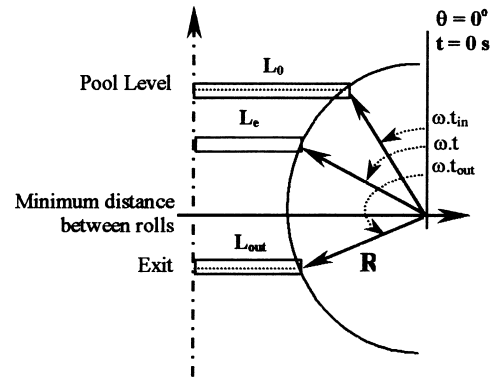


Fig. 5. Schematic diagram of the mathematical system used in the development of the proposed model.

### 2.5. Numerical grid

By considering the system presented in Fig. 2, the mathematical expressions for the boundary conditions can be expressed as follows:

$$L_e = R[1 - \sin(\omega t)] + \frac{e_0}{2} \quad (24)$$

where  $L_e$  is the effective length of the pool ( $\omega t$ ),  $t$  the time, and  $\omega$  is the rotational speed of the rolls.

It can be seen in Fig. 5 that the pool length ( $L_e$ ) must vary between an initial time ( $t_{in}$ ) up to an outlet time ( $t_{out}$ ), which are defined at the interval:  $e_0/2 < L_e < L_0 = L_{cp}/2$ . Therefore, the effective length of the mesh have been defined as:  $L_{max} = L_0$ ;  $L_{min} = e_0/2$ ;  $L_{outlet} = e_0/2$ .

In the present analysis, the assumption for time equal to zero ( $t_0 = 0$ ) is given for a vertical direction at the roll center, and first calculated must be the initial time for the condition where the length of the pool is  $2L_0$ , given by

$$t_{in} = \arcsin \left[ \frac{(e_0/2 + R - L_0)/R}{\omega} \right] \quad (25)$$

The numerical system works with a uni-dimensional mesh, with constant size ( $\Delta x = \text{constant}$ ) and a heat-exchange surface,  $At = \Delta y \Delta z$ . The mesh size ( $\Delta y$ ) is proportional to the roll velocity, given by

$$\Delta y = \frac{Y_{in}}{N_y} \quad (26)$$

where  $Y_{in}$  is

$$Y_{in} = R \cos(\omega t_{in}) \quad (27)$$

and  $N_y$  is an inlet parameter of the model, that is associated directly with the system precision. The final time  $t_{out}$  is calculated from:

$$t_{out} = \arcsin \left[ \frac{(2R + e_0 - e_f)/2R}{\omega} \right] \quad (28)$$

where  $Y_{out}$  is expressed as

$$Y_{out} = R \cos(\omega t_{out}) \quad (29)$$

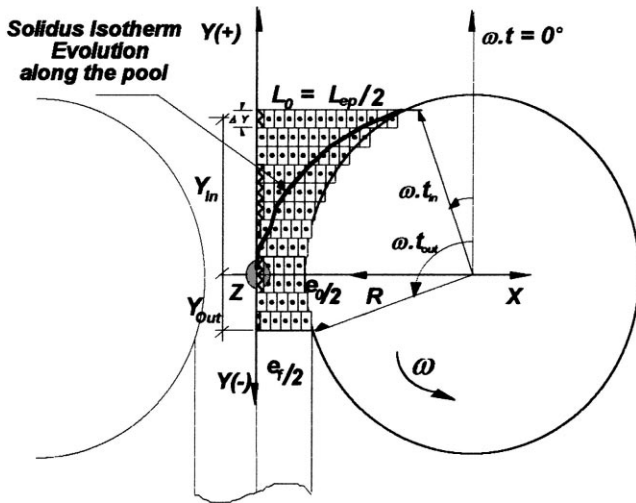


Fig. 6. Schematic diagram of the numerical grid.

The assumed numerical grid has 400 elements at the pool level, and was not kept constant during the process, as shown in Fig. 6.

### 3. Numerical results and discussion

The results that will be presented are concerned with the modeling of the “twin-roll” continuous casting process, encompassing the heat transfer and solidification analysis.

A one-dimensional version of the proposed model was used to simulate the evolution of the liquidus and solidus isotherms during the solidification process, as well as the cooling curves at specified points inside the metal. A first set of simulations were performed using a Sn–15%Pb alloy as the reference material. The physical properties of the alloy and the numerical model inlet parameters are presented, respectively in Tables 2 and 3 [8].

Figs. 7 and 8 present the results of liquidus and solidus displacements according to the numerical model compared to a model developed previously by Saitoh [8]. It can be seen that there is a good agreement between the proposed-model simulations and those from the literature.

Table 2  
Physical properties of Sn–15%Pb

Physical property	Unit	
Solid thermal conductivity	W/m K	50.2
Liquid thermal conductivity	W/m K	21
Solid specific heat	J/kg K	230
Liquid specific heat	J/kg K	250
Solid density	kg/m <sup>3</sup>	7200
Liquid density	kg/m <sup>3</sup>	7200
Latent heat	J/kg	159106
Liquidus temperature	°C	208
Solidus temperature	°C	183

Table 3  
Inlet parameters of the numerical model

Inlet parameter	Unit	
Roll diameter (copper)	mm	89
Temperature of roll cooled surface	°C	17
Thickness of the pool (plane XY)	mm	30
Width of the pool (plane YZ)	mm	100
Angle between the molten metal surface and the roll “outlet”	degree	43
Metal/roll heat-transfer coefficient	W/m <sup>2</sup> K	3000
Rotational speed of rolls	rad/s	0.72
Distance between the rolls	mm	3.25
Liquid metal temperature at the pool surface	°C	209

The main advantages of the proposed model are: (a) versatility and flexibility, permitting an easier manipulation of the heat-conduction equation and of physical properties variable with temperature in mushy zone; (b) the possibility of introducing any treatment concerning the latent-heat evolution along the liquid/solid interval (the model as proposed by Saitoh uses a linear evolution of latent heat in the mushy zone, and the numerical simulations of the proposed model have used Scheil’s equation, which is considered to give a more realistic description of the evolution of the latent heat for most substitutional solid solutions); and (c) the introduction of a finite metal/roll heat-transfer coefficient (constant or variable) instead of a fixed temperature boundary condition as used in Saitoh’s approach.

As shown in Fig. 8, the difference assumed in the evolution of the latent heat has a stronger influence on the predictions of the solidus isotherm displacement, the agreement between the two solutions not being good.

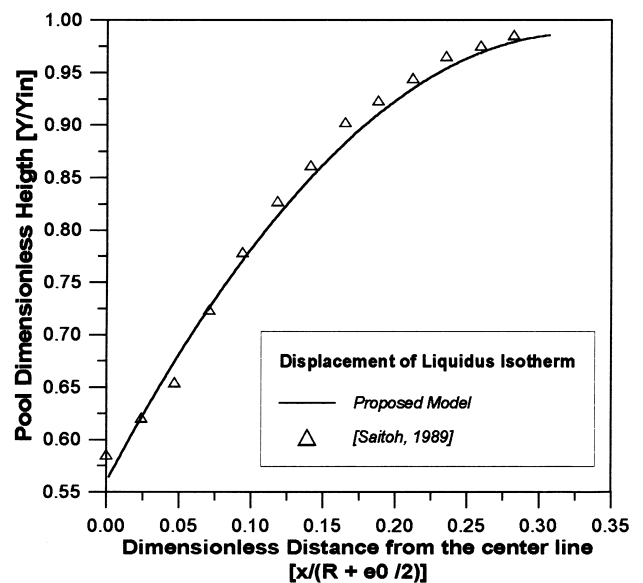


Fig. 7. Displacement of the liquidus isotherm: comparison between numerical model predictions and data from the literature for Sn–15%Pb.

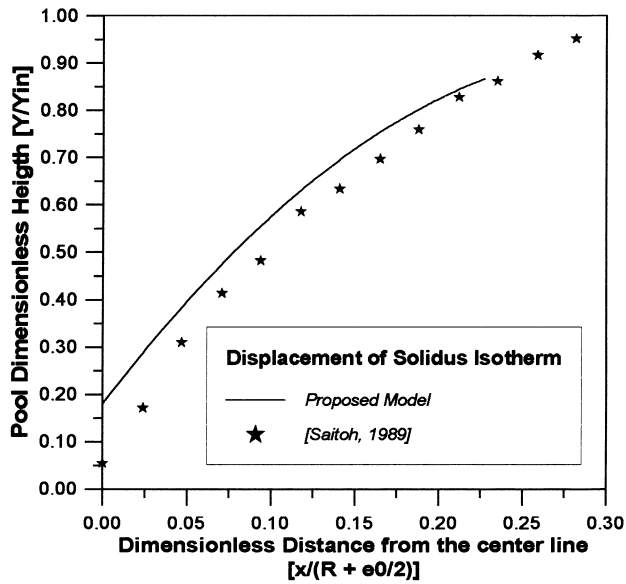


Fig. 8. Displacement of the solidus isotherm: comparison between numerical model predictions and data from the literature for Sn–15%Pb.

The metal/roll heat-transfer coefficient is of great importance in “twin-roll” continuous casting, since thin strip solidification is a casting process in which interface resistance is dominant.

To analyze the influence of such parameters on the evolution of solidification, Fig. 9 presents some simulations performed using the proposed model under different metal/roll heat-transfer efficiencies.

In order to analyse the model performance with a material of commercial interest in the production of thin strips,

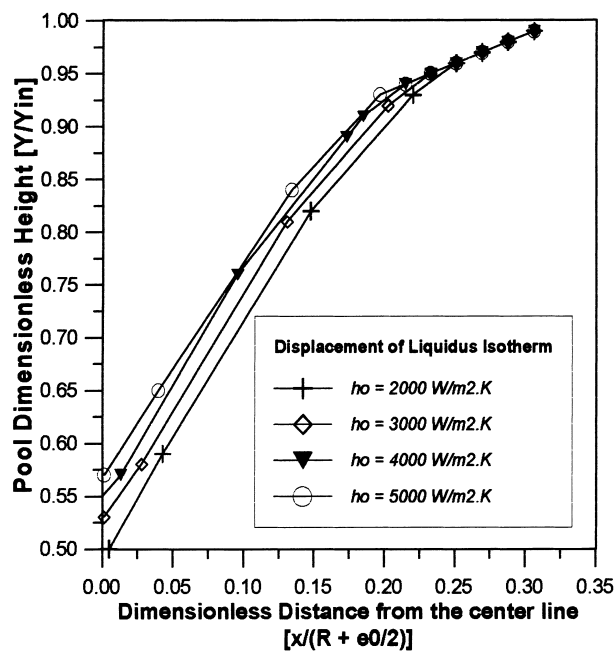


Fig. 9. Displacement of the liquidus isotherm as a function of metal/roll heat-transfer efficiency for Sn–15%Pb.

Table 4  
Physical properties of stainless steel

Physical property	Unit	
Solid thermal conductivity	W/m K	29.3
Liquid thermal conductivity	W/m K	20
Solid specific heat	J/kg K	679
Liquid specific heat	J/kg K	670
Solid density	kg/m <sup>3</sup>	7400
Liquid density	kg/m <sup>3</sup>	7600
Latent heat	J/kg	272000
Liquidus temperature	°C	1460
Solidus temperature	°C	1399

Table 5  
Inlet parameters of the numerical model

Inlet parameter	Unit	Stainless steel
Roll diameter (copper)	mm	230
Temperature of the cooled roll surface	°C	17
Thickness of the pool (plane XY)	mm	308
Width of the pool (plane YZ)	mm	100
Angle between the molten metal surface and the roll “outlet”	degree	70°
Metal/roll heat-transfer coefficient	W/m <sup>2</sup> K	5000
Rotational speed of the rolls	rad/s	0.1
Distance between the rolls	mm	10
Liquid metal temperature at the pool surface	°C	1500

stainless steel was used on model simulations. The stainless steel physical properties and the inlet operational parameters used in numerical simulations are presented respectively in Tables 4 and 5. Figs. 10 and 11 present the results concerning the evolution of the solidification of stainless steel strips as well as the evolution of the temperature of the metal and the surface of the copper roll during the process.

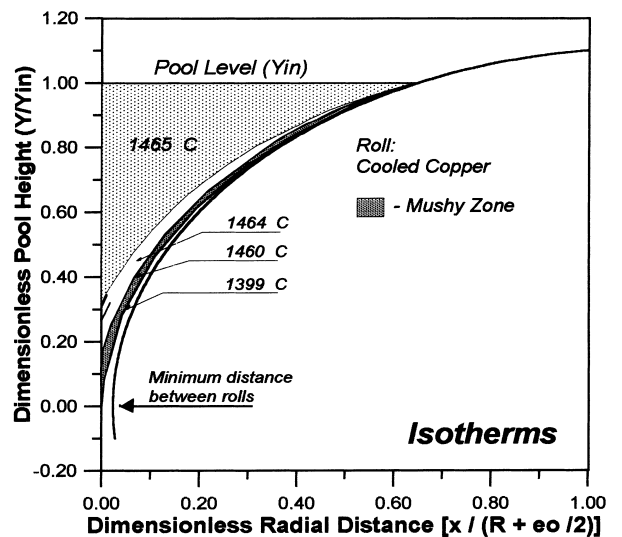


Fig. 10. The evolution of isotherms during the solidification of thin stainless steel strips.

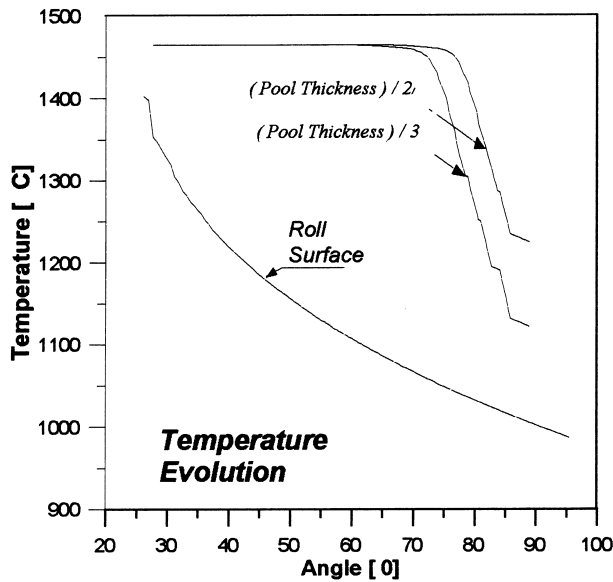


Fig. 11. Temperature evolution of metal/roll system during the process, where the metal is: stainless steel.

#### 4. Conclusions

The proposed model for the two-dimensional solidification problem in the “twin-roll” continuous casting system has proved to be efficient, versatile and of easy formulation, as can be seen by the results of simulations performed with the model. The numerical results have been compared with data from the literature to check the validity of the proposed method. The developed mathematical model should help in the rational design and control of “twin-roll” experimental systems.

#### 5. Nomenclature

$A$	area ( $m^2$ )
$C_T$	capacitance ( $J/K$ )
$c$	specific heat ( $J/kg\ K$ )
$e_0$	minimum distance between rolls (m)
$e_f$	final strip thickness (m)
$h_0$	metal/roll heat-transfer coefficient ( $W/m^2\ K$ )
$f_s$	solid fraction
$i, j$	mesh indices
$k$	thermal conductivity ( $W/m\ K$ )
$k_0$	equilibrium partition coefficient
$L$	latent heat of fusion ( $J/kg$ )
$L_E$	effective length (m)
$L_{EP}$	pool thickness in the $X$ – $Y$ plane (m)
$L_r$	pool width in the $Y$ – $Z$ plane ( $z$ -direction) (m)
$L_0$	pool thickness/2 (pool length/2) (m)
$n$	time index

$Pe$	Peclet number
$\dot{q}$	heat source
$R_{Roll}$	roll radius (m)
$R_T$	thermal resistance ( $K/W$ )
$T$	temperature (K)
$T_l$	liquidus temperature (K)
$T_f$	fusion temperature (K)
$T_v$	pouring temperature (K)
$t$	time (s)
$v$	velocity in $x$ and $y$ directions (m/s)
$V$	volume ( $m^3$ )
$x, y, z$	coordinate system
$Y_{IN}$	pool height ( $y$ -direction) (m)
$\rho$	specific mass (density) ( $kg/m^3$ )
$\omega$	rotational speed of the rolls (rad/s)

#### Acknowledgements

The authors would like to acknowledge the financial support provided by FAPESP (The Scientific Research Foundation of the State of São Paulo), FINEP-RECOPE and IPT (Technology Research Institute) São-Paulo, Brazil.

#### References

- [1] J.K. Brimacombe, I.V. Samarasekera, Fundamental aspects of the continuous casting of near-net-shape steel products, Proc. Int. Symp. On casting of near-net-shape products, Y. Sahai, J.E. Battles, R.S. Carbonara and C.E. Mobley, eds. The Metallurgical Society, Warrendale PA (1988) 3.
- [2] X. Liang et al., Edge containment of a twin-roll caster for near-net-shape strip casting, J. Mater. Process. Technol. 63 (1997) 788.
- [3] B.Q. Li, Producing thin strips by twin-roll casting. Part I: Process aspects and quality issues, J. Min. Met. Mater. Soc. (1995) 13 (A).
- [4] R. Cook, P.G. Grocock, P.M. Thomas, D.V. Edmonds, J.D. Hunt, Development of the twin-roll casting process, J. Mater. Process. Technol. 55 (1995) 76.
- [5] M.J. Bagshaw, J.D. Hunt, R.M. Jordan, Heat line formation in a roll caster, Appl. Sci. Res. 44 (1987) 161.
- [6] K. Miyazawa, J. Szekely, A Mathematical model of the splat cooling process using the twin-roll technique, Metall. Trans. A 12A (1981) 1047.
- [7] B.Q. Li, Producing thin strips by twin-roll casting. Part II: Process modeling and development, J. Min. Met. Mater. Soc. (1995) 13 (B).
- [8] T. Saitoh, H. Hojo, H. Yaguchi, C.G. Kang, Two-dimensional model for twin-roll continuous casting, Metall. Trans. B 20B (1989) 381.
- [9] B.S. Berg et al., Gauge reduction in twin-roll of an AA5052 aluminum alloy: the effects on microstructure, J. Mater. Process. Technol. 53 (1995) 65.
- [10] H.G. Kraus, Finite-element model and feasibility study of thin strip continuous casting of steel, Numer. Heat Transfer 10 (1986) 63.
- [11] V.R. Voller, C.R. Swaminathan, General source-based method for solidification phase change, Numer. Heat Transfer B 19 (1991) 175.
- [12] J.A. Spim Jr., A. Garcia, An optimization of the finite difference method for modeling solidification of complex shapes, J. Braz. Soc. Mech. Sci. 19 (1997) 392.